Chapter 3

Structural Basis & Protein-Protein Interaction Studies of RAP80

3.1 Introduction

Cells have evolved a complex, dynamic and highly regulated network, called DNA damage response (DDR), to achieve extreme fidelity. In genotoxic stress, DDR coordinates numerous cellular processes like cell-cycle regulation, chromatin-remodeling, DNA-repair and transcriptions [20]. Sensing the DNA damage and promulgation of the DDR signaling cascade involve recruitment and assembly of many DDR mediators and effectors at the sites of damage [35, 147]. Double strand breaks elicit the activation of ATM and ATR kinases, which phosphorylate histone variants H2AX and MDC1 [17, 35, 86, 87, 148-150]. This event endorses the assembly of DDR mediators, which in turn facilitates the recruitment of UBC13/RNF8 to the DNA damage site [88, 151-153]. In the signaling pathways, this leads to the formation of polyubiquitin chains on H2AX, which are recognized by RAP80 (**Figure 3.1**) [17, 87, 149, 150]. RAP80 has two tandem UIM (Ubiquitin-Interacting Motif) at its N-terminal, ABRAXAS (CCDC98) Interacting Region (AIR) at the central domain, and two zinc -finger domains at its C-terminal [108]. It has been reported that RAP80 forms a stable complex with BRCA1 through an intermediate binding partner CCDC98 [6, 7, 16]. CCDC98 has a consensus sequence S-X-X-F motif at its C-terminus, which is involved in interactions with phospho-specific binding domain of BRCA1-BRCT [2, 6-8].

RAP80 acts upstream of CCDC98 and BRCA1 in DDR, and is required for the localization of the BRCA1 complex to ionizing radiation (IR)-induced foci (IRIFs)[6, 16, 112]. RAP80 knockdown cells have shown hypersensitivity to IR and ultraviolet (UV) light, cell -cycle dysfunction and defective homologous recombination (HR) repair [6, 7, 16, 87]. RAP80 and p53 auto-regulate each other and have influence on apoptosis [154].

Loss of RAP80 alleles (RAP80 $^{-/-}$) increase the susceptibility to lymphoma, and promote tumor development in both p53$^{-/-}$ and p53$^{-/+}$ mice [155]. UIM1 and UIM2 motifs of RAP80 are very crucial since deletion of either or both motifs significantly perturb the foci formation of RAP80-BRCA1 complex at the DNA damage site [5].

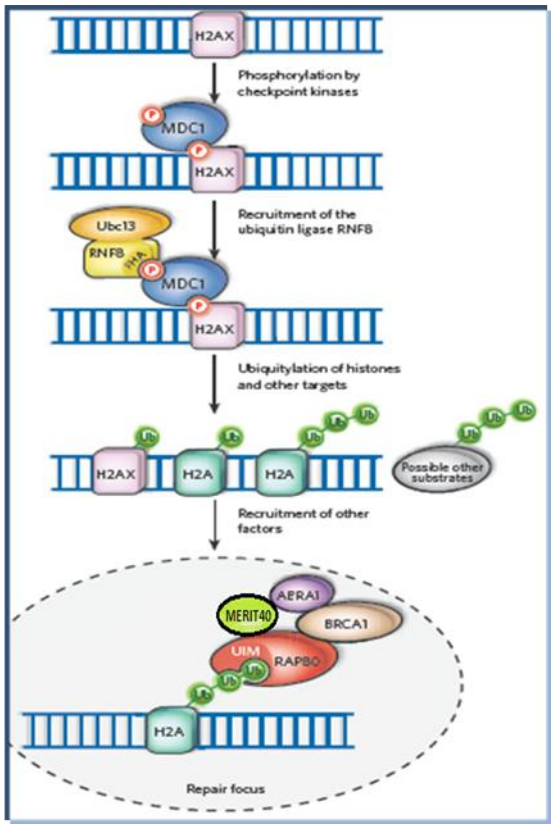

Figure 3.1: DNA damage response in repair pathway.

A novel alteration, c.241-243delGAA (ΔE81), which leads to an in-frame deletion of glutamic acid residue, has been identified at UIM1 motif of RAP80 [5]. RAP80 ΔE81 variant has been discovered in patient diagnosed with breast cancer, and the residue is found to be highly conserved among all the vertebrates. This variant showed an observed frequency of 0.9% (1/112) in the familial cases compared to 0.3% (1/325) in the controls (P¼0.45; OR¼2.92; CI¼0.18–47.1). Another RAP80 ΔE81 carrier was also diagnosed with bilateral breast cancer in a group of 503 breast cancer cases (0.2%, 1/503) [5].

Furthermore, RAP80 ΔE81 expressing cells have shown abrogation of DSB localization of the RAP80–BRCA1 complex, and exhibited genomic instability (chromosomal aberration) [5].

A comparative structural stability and binding analysis of RAP80 (1-130) wild- type and RAP80 (1-130) ΔE81 was carried out to understand the functional implication(s) of this mutation. Our main goal is to analyze the structure of wild-type and functionally important mutants of RAP80 and its binding partners. The aim here is to use biophysical, biochemical and structural biology tools to disentangle the convolution of RAP80-BRCA1 complex.

3.2 Material and Methods

A comparative structural, stability and binding analysis of RAP80 (1-130) wild-type and RAP80 (1-130) ΔE81 was carried out. Different functional domains of RAP80 were sub-cloned in pGEX-kT vector (Amersham Pharmacia) as shown in figure 3.2. RAP80 (1-130) wild-type, RAP80 (1-130) ΔE81 and RAP80 (1-405) were sub-cloned from the mammalian vector (pEGFP-c1, a kind gift from J. Chen, USA) to the bacterial expression vector using one step cloning method. The basic scheme for sub-cloning, and nucleotide sequence of primers used in PCR reaction are shown in **Figure 3.3**. The gene of interest was amplified using following PCR condition: 95 °C denaturation (5 minutes), 95 °C denaturation (45 seconds), annealing 65°C for 35 seconds, extension 72°C at 0.5kb/min, final extension 72°C for 10 minutes, 25 cycles. The PCR amplified product was digested with EcoR1 and BamH1 and ligated in the pGEX-kT vector (a kind gift from J. Ladias laboratory). The ligation mixture was transformed into *E.coli* DH5α cells. Colony screening was done by insert release from the plasmid using EcoR1 and BamH1

restriction enzymes and further confirmed by DNA sequencing. Positive clones were used for protein expression and purification.

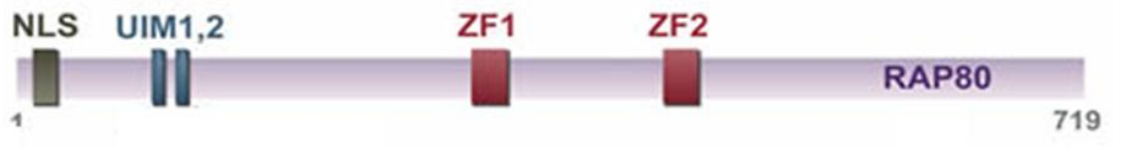

Figure 3.2: Different functional domains of RAP80

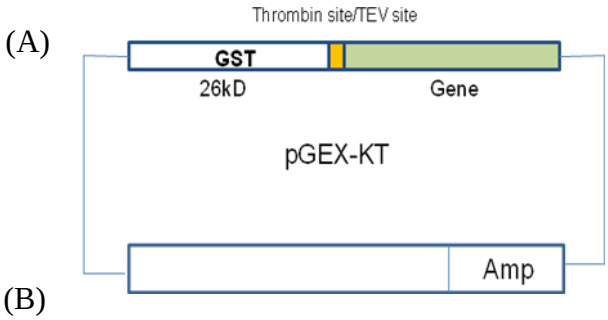

GTC	BamH1	TEV	ATGCTGATCCGATTCTACTACCTTATCCAAGG
GTC	EcoR1	STOP	TCT GGT AGC GGA AGC ATC AGA AGG CCG GCA AC

Figure 3.3: Basic scheme of sub-cloning of different functional domain of RAP80 in pGEX-kT. (A) Vector construct. (B) RAP80 primers used during PCR amplification.

RAP80 (1-130) wild- type and RAP80 (1-405) were expressed in bacterial system *E.coli* BL21 (DE3) cells. For protein expression, 100 µg/µl plasmid construct was transformed into *E.coli* BL21 (DE3) cells and grown on LB agar plate containing antibiotic ampicillin (100 µg/ml). Detailed protocol is described below.

Protocol for protein expression:

1. **Inoculation:** Pick-up a single transformed colony from antibiotic resistant LB agar plate and inoculate it in 100 ml LB broth containing 100 µg/ml of ampicillin. Incubate on shaker incubator at 37^{o}C overnight.

2. **Dilution:** Inoculate 10 ml of starting culture to 1000 ml (1: 100 ratios) of autoclaved LB broth containing 100 µg/ml of ampicillin. Incubate the flasks on shaker incubator at 37 ^{o}C until it has reached mid-log phase i.e. A_{600} between 0.6-0.8.
3. **Induction:** Cool down the flasks and add 400 µl IPTG (stock 1M) and incubate on shaker incubator at 24^{o}C for 16 hours.
4. **Harvesting:** The culture was transferred to centrifuge bottles and centrifuged for 10 minutes at 6000 rpm at 4^{o}C. The pellet was resuspended in a small amount of supernatant and centrifuged for 15 minutes at 5000 rpm, 4 ^{o}C.
5. **Storage:** The pellet obtained can be stored at -80 ^{o}C for further use.

Proteins were purified by affinity chromatography followed by FPLC. RAP80 (1-130) ΔE81 mutant was expressed in *E.coli* (BL21) and purified as per wild- type protocol.

Protocol for purification of RAP 80 and ΔE81:

Purification buffer composition: 10 mM HEPES (pH 7.5), 300 mM NaCl, 0.1 mM EDTA, 2 mM β-ME, 5% ethylene glycol pH 7.5

FPLC buffer composition: 10 mM HEPES (pH 7.5), 300 mM NaCl, 0.1 mM EDTA, 2 mM BME pH 7.5

1. **Re-suspension**: Re-suspend the pellet of RAP80 in 40 ml of purification buffer; supplemented with 200 mM PMSF and 20µl of protease inhibitor.
2. **Ultra sonication**: Transfer the suspension into centrifuge tube and sonicate at 50 pulse rate and 50 power with 1.45 minutes of duty cycle.
3. **Centrifugation:** After sonication, the suspension was subjected to centrifugation at 18000 rpm for 45 minutes at 4^{o}C to obtain cleared lysate. Collect the supernatant and discard.

4. **Binding**: The soluble fraction obtained is brought to room temperature and then mixed with pre-equilibrated affinity resin and incubated at room temperature for 1 hour. The sepharose beads in affinity column charged with glutathione binds specifically to those proteins having GST (Glutathione-S-transferase) tag.
5. **Washing**: After binding, the column is given 4 column washes with wash buffer so as to remove any non specific protein.
6. **Cleavage**: Add 400 µl of TEV protease, 40 µl of protease inhibitor cocktail and 100 µl of PMSF in 20 ml of purification buffer and perform the cleavage step for 3 hours by passing the solution through column at interval of 1 hour. Take out 40 µl of beads to observe the cleavage of protein.
7. **Elution**: After TEV cleavage the protein is eluted with 30 ml of purification buffer.
8. **Equilibration of Ni-NTA resin**: Give 2 column washes with double distilled water and then 5 to 6 column washes with wash Buffer.
9. **Metal Ion Chelate Affinity Chromatography**: After calibration of Ni-NTA resin, pass the eluted fractions through them to get rid of His-tagged TEV protease contaminant.
10. **Concentrating the protein:** Transfer the eluted protein in a 10 kDa pre-equilibrated centricon and concentrate the protein upto 2 ml by centrifuging it at 4500 rpm for 10 minutes at 4 ^{o}C. Check the concentration on Nanodrop spectrophotometer (280 nm). Centrifuge for 10 minutes at 13000 rpm at 4 ^{o}C for removal of insoluble aggregates or precipitates.
11. **Gel filtration:** Inject 2 ml of concentrated protein in AKTA- FPLC against FPLC buffer.

12. **Fraction collection**: Collect the purified protein obtained through FPLC in 1.7 ml eppendorf at its elution volume according to gel filtration spectra profile of the sample.
13. **Loading on SDS-PAGE 12% gel**: Load 20 µl of FPLC fractions on SDS-PAGE, stain with commassie dye, and then destain it to visualize the protein of interest.
14. **Concentrate the protein**: The fractions which showed purified protein band was further concentrated as per the requirement.

The purified proteins were used in various bio-physicochemical experiments. In addition, binding analysis of RAP80 (1-405) was performed with its binding partner. The complete details of protocol have been discussed in chapter 3 (Material and Methods).

3.3 Results and discussion

3.3.1 Cloning, expression and purification of RAP80 functional domain: Selected potential clones when digested with the EcoR1 and BamH1 restriction enzymes showed the insert release of appropriate size (**Figure 3.4**). Sequencing results confirmed the presence of ligated gene of interest in the vector with desired frame of codon sequence.

RAP80 (1-130) wild-type and mutant eluted at the same elution volume (98 ml) corresponding to monomer (**Figure 3.5**). This indicates that RAP80 ΔE81 mutation does not change its oligomeric property. However, the elution profile of RAP80 (1-405) showed that most of the protein is oligomeric in nature and forms aggregates. Very minuscule amount of RAP80 (1-405) protein was observed at proper elution volume (corresponding to monomer).

3.3.2 Structural insight into RAP80-Ub complex using *in-silico* analysis: In order to analyze the structural changes due to RAP80 mutation (ΔE81), RAP80 (80-120) ΔE81

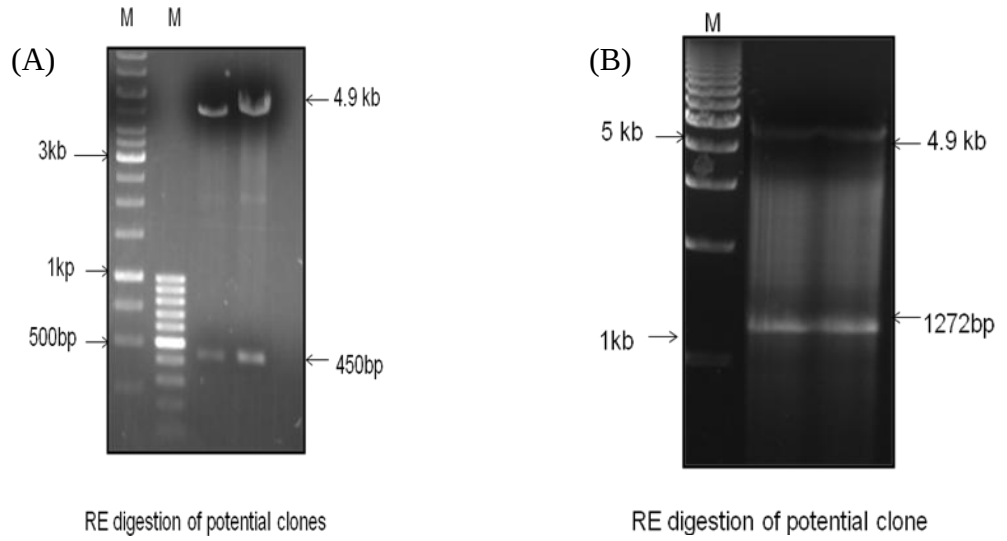

Figure 3.4: Agarose gel showing the insert release from potential clones' plasmids; (A) pGEX-KT-rap80 (1-130), (B) pGEX-KT-rap80 (1-405).

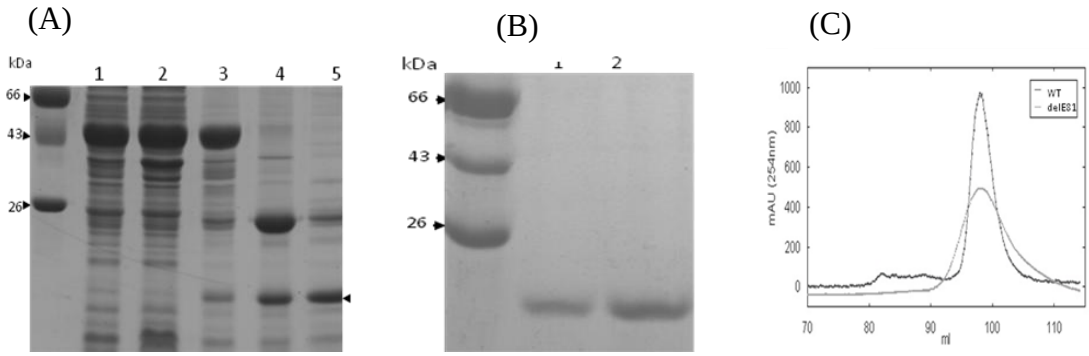

Figure 3.5: Expression and purification profile of RAP80 (1-130). (A) Lane 1-Total protein, 2-soluble protein, 3-fusion protein bound on beads, 4- protein after on beads cleavage and 5-elution fraction of affinity purified protein. Single arrow - RAP80 (1-130) protein, (B) Purified protein after gel filtration chromatography on SDS-PAGE. Lane 1- RAP80 (1-130) delE81, 2- RAP80 (1-130) wild-type(C)-Overlay of gel filtration spectra of RAP80 wild-type and ΔE81 (Superdex 200) [156].

functional motif (called as UIM) was modeled using homology modeling server (Swiss Modeller, www.swissmodel.expasy.org/) considering, RAP80-Ub NMR structure (PDB ID: 2RR9) as the template [12]. A model was selected based on good stereo chemistry and better Ramachandaran plot. The model was further validated using server "**SAVES**" (Metaserver for analyzing and validating protein structures, http://nihserver.mbi.ucla.edu/SAVES/).

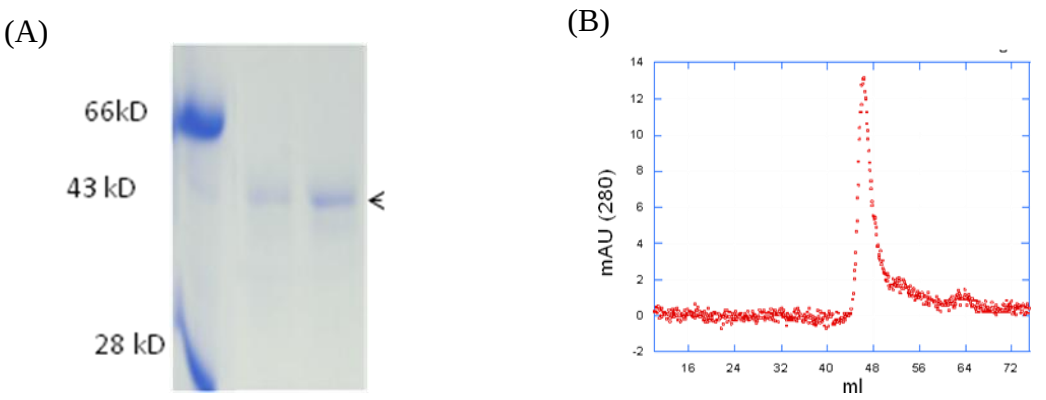

Figure 3.6: Purification of RAP80 (1-405). (A) Purified protein represented by single arrow head. (B) The gel filtration spectra of the same.

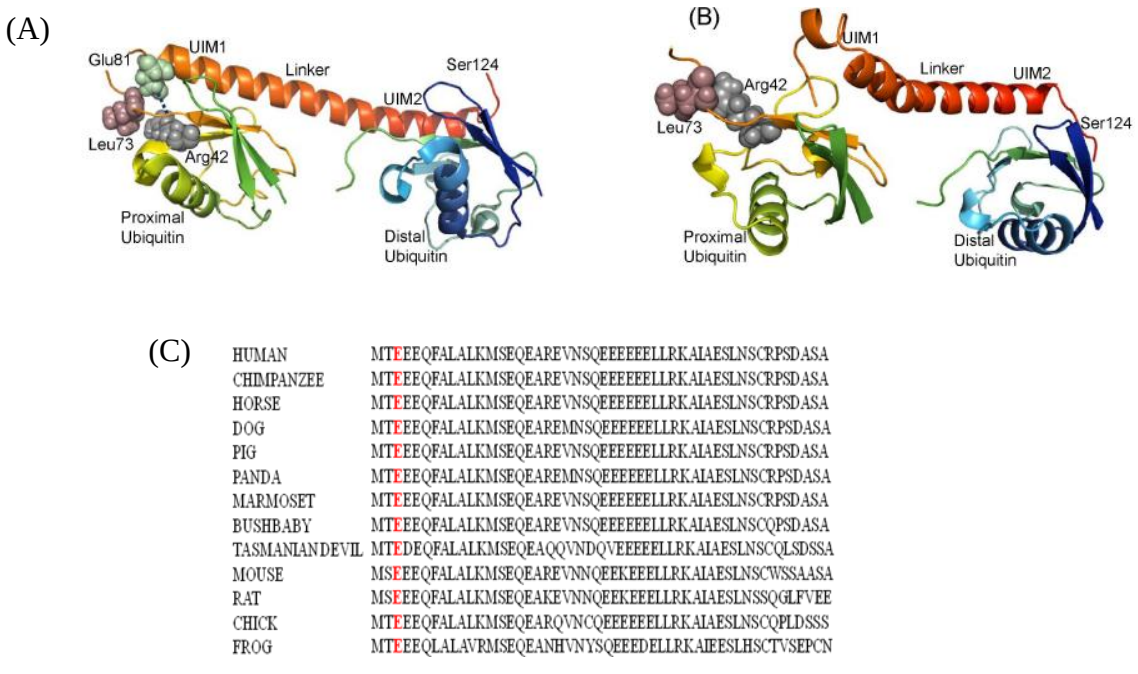

Figure 3.7: Binding interaction of RAP80 UIMs and ΔE81 with Di-Ub (K-63 linked). (A) Structure of Di-Ub (K-63 linked)-RAP80 UIMs (79-124) wild-type (PDB ID: 2RR9), and (B) Di-Ub (K-63 linked)-RAP80 (79-124) UIMs ΔE81. (C) Multiple sequence alignment of UIMs region showing Glu 81 residue highlighted in red color [156].

The server SAVES mainly comprises of five programs, Procheck, What_check, Errat, Verify_3D and Prove. The modeled structure was simulated for 5 ns using Desmond software (Schrodinger) and superimposed on wild- type complex. PDBsum software was used to analyze the interactions [157].

Modeled structure revealed that UIM1 and UIM2 motifs are connected with a linker in a head-to- tail manner. The three-dimensional structure of the wild-type was predominantly α-helical in nature and approximately 59 Å long . Strikingly, in case of ΔE81 mutant, α–helix is partly distorted and shortened to 45 Å. UIM1 and UIM2 bind to their respective proximal and distal ubiquitin of Di-Ub (K-63 linked) in 1:1 affinity ratio [158, 159]. Glu residue at 81 position was found to be highly conserved (**Figure 3.7**) and forms ionic bond and hydrophobic interaction with Arg42 and Leu73 residue of proximal ubiquitin, respectively. However, a drastic conformational change in RAP80 UIMs ΔE81 was found which significantly altered the intermolecular interactions with ubiquitin. Structural distortion in RAP80 UIMs ΔE81 probably renders its binding interactions unfavorable with Di-Ub (K-63 linked).

3.3.3 Structural insights into RAP80-Ub complex using *in-vitro* analysis: In order to determine the domain stability of RAP80 (1-130) wild-type and ΔE81 against the protease digestion, limited proteolysis was performed using trypsin and chymotrypsin. After treating the wild-type and mutant for limited time period with equal enzyme concentration, it has been observed that domain stability of RAP80 (1-130) wild-type is significantly higher than that of ΔE81. This imply that wild-type exists in a well formed structure which made it resistive towards protease digestion (**Figure 3.8**). However, high susceptibility of ΔE81 towards protease digestion indicates its probable deformed structure.

Susceptibility towards limited proteolysis of RAP80 (1-130) ΔE81 impart the supposition of deformities in the native structure. Hence, the secondary structural components with far-UV Circular Dichroism were investigated (**Figure 3.9**). RAP80 (1-

130) wild-type showed an estimated percentage of α-helices, β-sheets, turns and random structure as 45, 13, 16, and 26 % respectively, while for ΔE81 the corresponding values were 5.1, 4.7, 3.2 and 88 %. It suggests that secondary structural component of RAP80 is severally altered due to mutation, resulting in the loss of α-helical characteristic. β-sheet proportion was also moderately altered, and the mutant showed majority of random coil structure. Earlier report suggests that UIMs motif of RAP80 is found in equilibrium between α-helix and random structure [160]. ΔE81 mutation probably alters the α-helical conformation of RAP80 UIMs which leads to a shift in the equilibrium towards a random structure pattern.

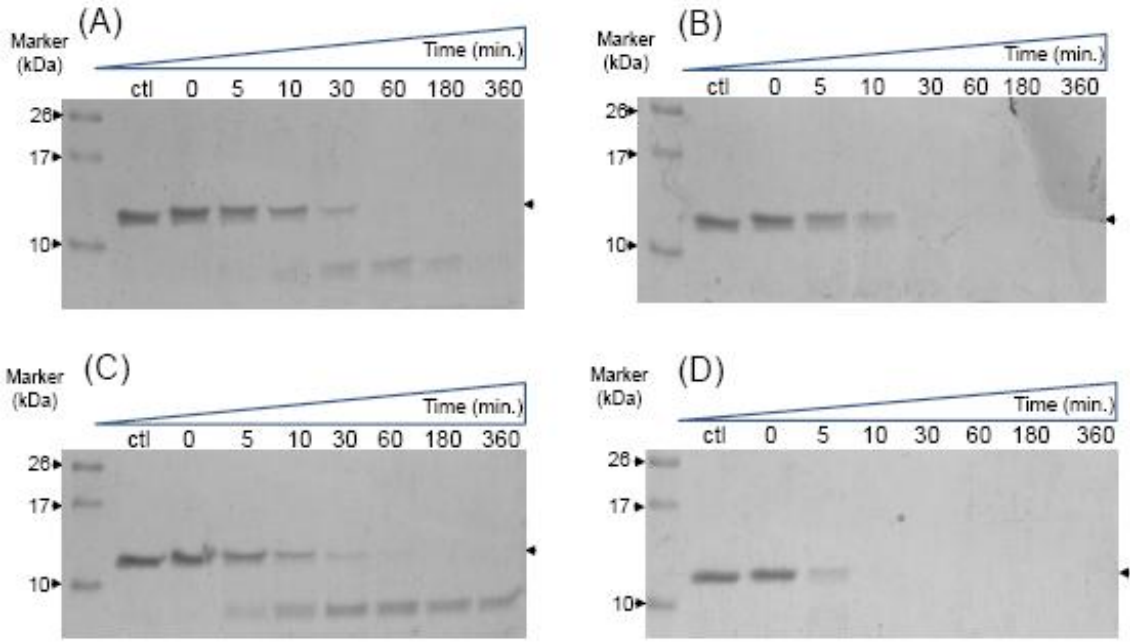

Figure 3.8: Resistivity profiles of RAP80 wild-type and ΔE81 towards protease digestion. Limited proteolysis of RAP80 wild-type (A, C) and ΔE81(B, D) using trypsin (A, B) and Chymotrypsin (C, D) as proteases. Ctl- control was taken as untreated with proteases [156].

Since limited proteolysis and Far-UV spectra deciphered changes in structural organization of ΔE81, it would be interesting to explore the domain stability and three dimension folding profile of wild-type and the mutant. Stability profiles of RAP80 wild-

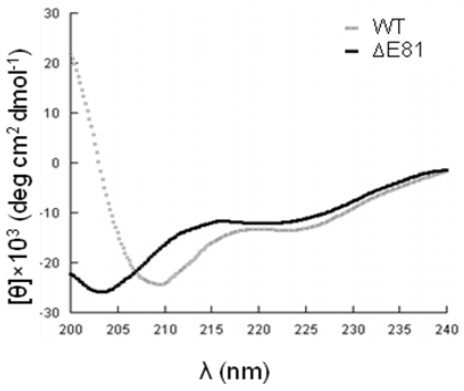

Figure 3.9: Comparison of secondary structural components of RAP80 (1-130). Overlay of Far-UV Circular Dichroism spectrum of wild-type and ΔE81.

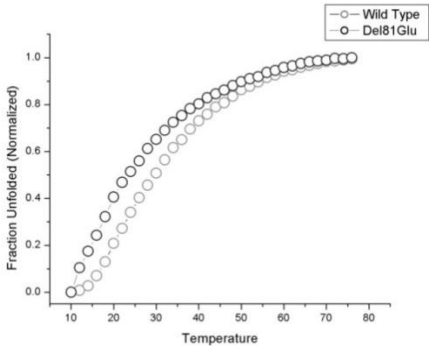

Figure 3.10: Thermal stability of RAP80 (1-130). Thermal denaturation of RAP80 (1-130) wild-type and ΔE81 in Circular Dichroism [156].

type and ΔE81 were compared at secondary (CD) and tertiary (DSC) structure levels. The spectra obtained from Circular Dichroism corresponding to λ at 218 nm showed the maximum changes in ellipticity and high signal to noise ratio **(Figure 3.10)**. Thermal stability of RAP80 ΔE81 (T_m 22°C, $\Delta G°_{H2O}$ 1.3±0.2 Kcal/mol, ΔH 1.0±0.5 Kcal/mol) was found significantly low compared to wild -type (T_m 29°C, $\Delta G°_{H2O}$ 2.0±0.5 Kcal/mol, ΔH 5.0±2.0 Kcal/mol) **(Figure 3.10)**. Thus, protein most likely unfolds without any intermediate species.

These findings were further supported by Differential Scanning Calorimetry, which gave a Tm value of 28°C for RAP80 wild-type **(Figure 3.11)**. However, a defined transition

for ΔE81 could not be obtained due to lesser stability and saturation concentration. Collectively, these results suggest that three-dimensional folding of RAP80 ΔE81 is impaired which may be due to helix to random structure transition of UIMs. ΔE81 mutation probably shifts this transition equilibrium towards the random structure.

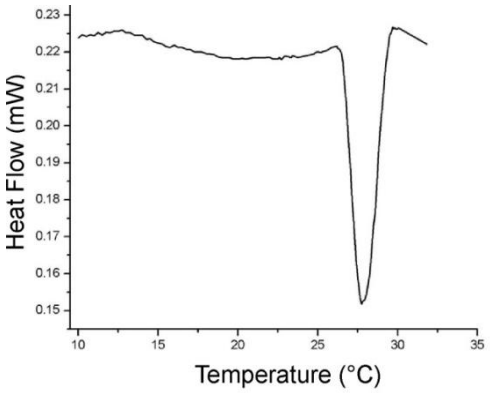

Figure 3.11: Differential Scanning Calorimetry profile of RAP80 wild-type [156].

3.3.4 Binding interaction of RAP80 wild-type and ΔE81 with di-Ub (K-63 linked): It is well reported that RAP80 UIMs bind to K-63 linked polyubiquitin chain(s) on the H2AX and recruit the RAP80-BRCA1 complex at the DNA damage site [6, 112]. Considering alterations in folding pattern & domain stability of RAP80 ΔE81, it can be suspected that it would further impair the binding affinity to the polyubiquitin chain. Binding analysis between RAP80 wild-type and ΔE81 with Di-Ub (K-63 linked) was performed using Surface Plasma Resonance (SPR) and GST pull-down assay. The observed binding affinity for RAP80 ΔE81 (K_D: 0.459 μM) was several fold less as compared to wild-type (K_D: 36.5 nM) in SPR **(Figure 3.12).**

GST pull-down assay also corroborated with the findings obtained using SPR **(Figure 3.12)**. Collectively, it can be concluded that RAP80 wild-type has higher binding affinity for the polyubiquitin chain, besides, it associates faster than ΔE81. Mutant protein

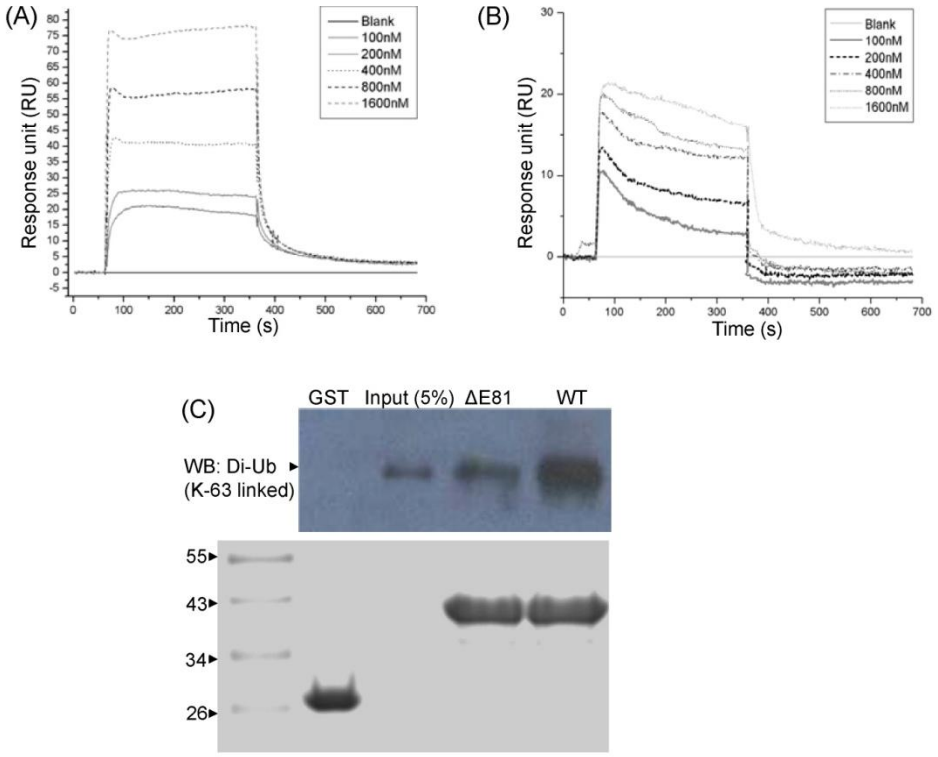

Figure 3.12: Binding analysis of RAP80 wild-type and ΔE81 with Di-Ub (K-63 linked). Sensograms of RAP80 wild-type (A) and ΔE81 (B) determined by Surface Plasma Resonance. (C) GST pull-down assay followed by western blotting. GST-RAP80 wild-type and ΔE81were used as a bait and Di-Ub (K-63 linked) as prey [156].

complex ΔE81-Di (Ub) is not stable due to high dissociation rate and lower binding affinity, which may be due to its structural deformation.

3.4 Crystallization of functional domain of RAP80

Protein crystallization was performed using commercially available reagents from Hampton Crystal Screen 1, 2 and SaltX screen. We tried both the hanging and sitting drop vapor diffusion methods. Initial crystallization trials for RAP80 (1-130) protein was set with 5 mg/ml protein concentration. The protein and mother liquor solution was mixed in 1:1 ratio (1 µl+1µl) and allowed to equilibrate at 22°C with 500 µl reservoir solution. Unfortunately, RAP80 (1-130) protein could not be concentrated more than 5 mg/ml due to high precipitation. A clear drop or light precipitation was observed in most

of the drops. Some crystallization conditions were selected for optimization on the basis of crystal conditions observed but all the effort for crystallization were futile. Crystal trial for mutant protein could not be performed due to its lower stability (0.2 mg/ml).

3.5 Conclusion

RAP80 wild-type and ΔE81 are moderately soluble proteins with a molecular weight of about 14 kDa. Thermal and proteolytic stability of wild -type was found to be significantly higher as compared to ΔE81, but both unfold via two-state transition. RAP80 UIMs are found in an equilibrium between random-coil and helical structure. Dynamic nature of UIMs provides immense flexibility for dissociation and association of ubiquitin molecules during the protein trafficking process.

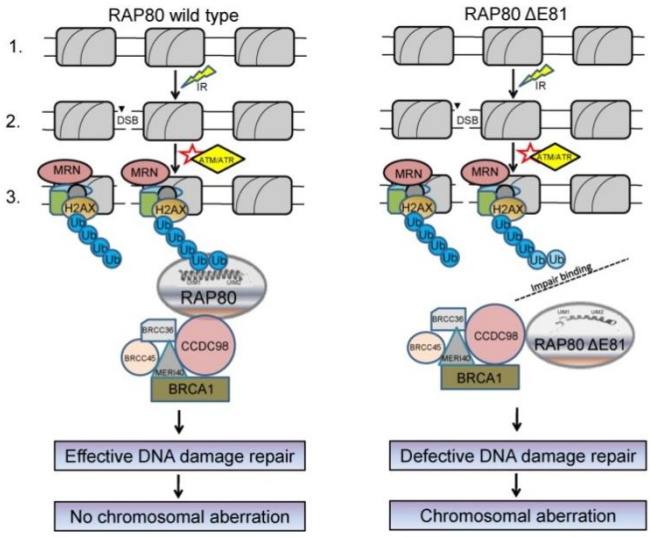

Figure 3.13: Mechanism of consequence for RAP80 wild type and ΔE81. The model elucidates mechanisms of chromosomal aberration due to RAP80 ΔE81 mutation. In the wild-type RAP80: **Step1**, showed the intact nucleosome complex; **Step 2**, double strand break due to ionization radiation; **Step 3**, ATM/ATR kinase activation and assembly of various damage repair proteins at DNA double strand break (DSB) site followed by formation of polyubiquitin chain(s) on histone(s) (H2AX) [156].

This dynamic nature is essential for a flexible and transient initiation mechanism of the DNA damage repair process. Deletion of 81E residue alters the helical conformation, thus shifting the equilibrium towards a random structure. Helical to random structure

transition results in the loss of weak intermolecular hydrogen bonds and hydrophobic interactions between the UIMs and Di-Ub (K-63 linked), thereby making the binding interactions unfavorable for ubiquitin. Since binding affinity of individual UIM for mono-ubiquitin is low [161], an avidity-based mechanism may play a very important role in the interaction between RAP80 and Lys 63-linked polyubiquitin. Co-operative binding between multiple UIMs and ubiquitin chains likely occurs, which may favor the interaction of second UIM with ubiquitin after positioning of the first [159]. It has been reported [5] that expression of RAP80 ΔE81 allele abates the recruitment of BRCA1 complex at DSB site, which further augments chromosomal aberration (chromatic breaks). Deletion of 81 glutamic acid residue significantly obliterates RAP80 structure and impairs its binding with the polyubiquitin chain. The unstable nature of mutant and di-ubiquitin complex may be responsible for defective recruitment of RAP80-BRCA1 complex to the DNA damage sites. Defective DNA damage repair perhaps leads to chromosomal aberration as shown in the model **(Figure 3.13).** Comparison of RAP80 ΔE81 with wild-type will help in understanding its role in various diseases and repair defects. It will further explore the possibility of structure based inhibitor design for therapeutic application that can compensate the effect of such mutations.